01 Apr 2008

Further Results on Frequency-Domain Channel Equalization for Single Carrier Underwater Acoustic Communications

Y. Rosa Zheng
Missouri University of Science and Technology, zhengyr@mst.edu

Chengshan Xiao
Missouri University of Science and Technology, xiaoc@mst.edu

Xin Liu
Missouri University of Science and Technology, xinliu@mst.edu

Wen-Bin Yang

et. al. For a complete list of authors, see https://scholarsmine.mst.edu/ele_comeng_facwork/1057

Recommended Citation

Y. R. Zheng et al., "Further Results on Frequency-Domain Channel Equalization for Single Carrier Underwater Acoustic Communications," *Proceedings of the MTS/IEEE Kobe Techno-Ocean, OCEANS 2008*, Institute of Electrical and Electronics Engineers (IEEE), Apr 2008.
The definitive version is available at https://doi.org/10.1109/OCEANSKOBE.2008.4531074

Further Results on Frequency-Domain Channel Equalization for Single Carrier Underwater Acoustic Communications

Yahong Rosa Zheng†, Chengshan Xiao†, Xin Liu†, T. C. Yang‡, and Wen-Bin Yang‡*

†Dept. of Electrical & Computer Eng., Missouri University of Science and Technology, Rolla, MO 65409

‡Naval Research Laboratory, Washington, DC 20375

***Abstract*— A frequency-domain channel equalization and phase correction method was proposed in a previous work published in Oceans'07 conference, in which 10^{-4} BER performance was presented for fixed-to-fixed source/receiver channels. The method is improved by using minimum mean square error (MMSE) estimation in channel updates rather than least squares estimation. It is applied to moving-to-fixed channels in the AUVFest'07 ocean experiment where single-carrier wideband transmission was employed with quadrature phase shift keying modulation. The moving source channels exhibit higher Doppler shift and larger Doppler drift than the fixed-to-fixed channels. Therefore, the number of symbols required for initial phase estimation is increased from 2 to 8 symbols when the group-wise phase correction algorithm is applied to the moving sources. Thirty-six packets with data block length of 512 symbols have been processed and 34 of them achieved an uncoded Bit Error Rate (BER) lower than 10^{-2}. The overall uncoded BER performance of all 36 packets is 1.81×10^{-3} which is slightly higher than that of the fixed-to-fixed channels.**

I. Introduction

Acoustic communications over shallow water horizontal channels faces significant technical challenges due to limited bandwidth, excessive multipath delay spread, and severe Doppler drift. The available bandwidth for medium range communications is only several ten kilo Hertz. The multipath delay spread is usually on the order of 5–30 ms which causes the intersymbol interference (ISI) to extend over 20–300 symbols at a data rate of 2-10 kilosymbols per second. The Doppler shift is dependent on the relative motion between the source (transducers) and receiver (hydrophones), the dynamic motion of the water mass, and the varying sound speed, etc. In a fixed-to-fixed (source-receiver or receiver-source) channel, the Doppler shift is close to zero Hertz; while in a moving-to-fixed channel, the Doppler shift can reach 20 Hz due to the low speed of sound waves in water. The ratio of Doppler shift to carrier frequency is on the order of 10^{-3} to 10^{-4} in underwater channels. In contrast, this ratio in RF wireless channels is on the order of 10^{-7} to 10^{-9}. The severe Doppler shift causes not only rapid fluctuation in the fading channel response but also compression or dilation of signal waveforms. These make the high data-rate, coherent receiver of underwater communication systems much more complicated [1]-[6] than RF systems.

In our previous works, two channel equalization methods have been applied to ocean experimental data for single-carrier, single-input multiple-output (SIMO) systems. The time-domain method was tested by UNet'06 experiments [8] and the frequency-domain method was tested by the AUVFest'07 experiments [7]. Both methods obtained 10^{-4} Bit Error Rate (BER) for fixed-to-fixed channels where the average Doppler shift was close to zero and the instantaneous Doppler drift from the mean was within ± 2 Hz. We proposed a new group-wise phase correction algorithm to combat the phase rotation problem caused by the instantaneous Doppler drift in the channel. The new algorithm differs from the the symbol-wise Phase-Locked Loop (PLL) method [1] in that the new algorithm corrects the phase drift after the equalization and the group-averaged phase drifts are re-estimated adaptively at an interval depending on the channel variation. It also differs from the group-wise phase correction scheme used with the time-reversal method [5], the passive phase conjugate method [6], or the decision feedback equalizer [4]. The new algorithm utilizes a few pilot symbols in each data block for phase reference thus achieves robustness against channel estimation errors and noise effects. The new algorithm has been applied to SISO (single-input single-output) and SIMO (single-input multiple output) systems using the fixed-to-fixed experimental data. The uncoded BER performance of the SISO systems varies between 4×10^{-4} to 6% depending on the channel conditions. When two or more receive hydrophones are used, the uncoded BER performance improves significantly to the order of 10^{-4}.

For moving-to-fixed channels, however, the average Doppler shifts are on the order of 10–20 Hz which causes significant carrier frequency offset (CFO). Besides, the variation of the instantaneous Doppler shift is as large as ± 5 Hz imposing more difficulties on channel estimation and channel equalization. In this paper, we improve the frequency-domain channel estimation and equalization algorithm for severe Doppler shift channels by adopting minimum mean square error estimation for channel updates rather than the original least squares algorithm. The performances of the FDE algorithm are evaluated using the AUVFest'07 experimental data. Thirty-six packets with data block length of 512 have been processed and 34 of them achieved an uncoded BER lower than 10^{-2}. The overall BER performance of all 36 packets is 1.81×10^{-3} which is slightly higher than that of the fixed-to-fixed channels.

The following notations are used throughout the paper: su-

*Dr. W.-B. Yang is now with Information Technology Laboratory, National Institute of Standards and Technology, Gaithersburg, MD 20899.

978-1-4244-2126-8/08/$25.00 ©2008 IEEE

perscript $()^t$ denotes the transpose, $()^*$ denotes the conjugate, and $()^\dagger$ denotes the conjugate transpose. The operator $E()$ denotes statistical average. The matrix $\mathbf{F}_N$ is the normalized Fast Fourier Transform (FFT) matrix of size $N \times N$ whose (m,n)-th element is given by $\frac{1}{\sqrt{N}} \exp\left(\frac{-j2\pi(m-1)(n-1)}{N}\right)$.

II. The AUVFest'07 Experiment

The AUVFest'07 experiments were conducted off the coast at Panama City, Florida, USA, in June 2007. Two fixed ACDS platforms were placed 5.06 km apart in shallow water, as shown in Fig. 1. Transducers and hydrophone arrays were housed on the ACDS platforms, which performed experiments of fixed-to-fixed source and receiver, as shown in Fig. 2. Eight hydrophones were unequally spaced over 1.86 m on a vertical linear array. The hydrophone array was deployed at the bottom of the water with a depth of 20 m. A source onboard a towing boat moved around the ACDS receivers at an average speed of approximately 4 knots, *i.e.*, 2 m/s. The transducer was deployed at a depth of 12.5 m. The range between the moving source and the fixed receiver was 1 km to 3 km. The route of the moving source is shown in Fig. 3.

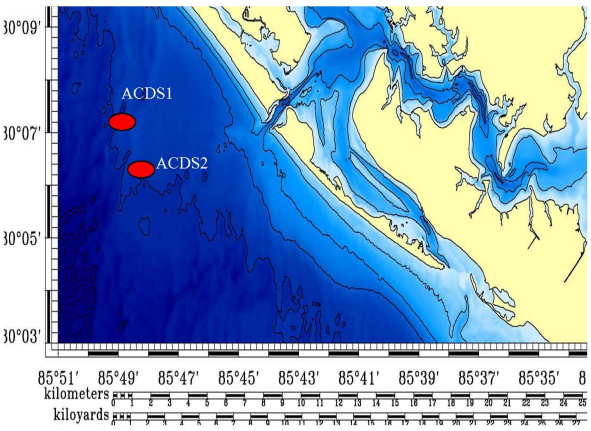

Fig. 1. Experiment site map. ACDS1 and ACDS2 indicate the locations of the two fixed receiver platforms.

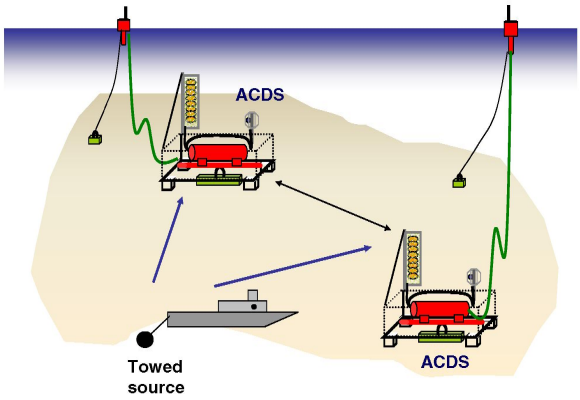

Fig. 2. Equipment setup of the experiment. The towed source moves around the two fixed receivers at a speed of 2 m/s with a range of 1–3 km.

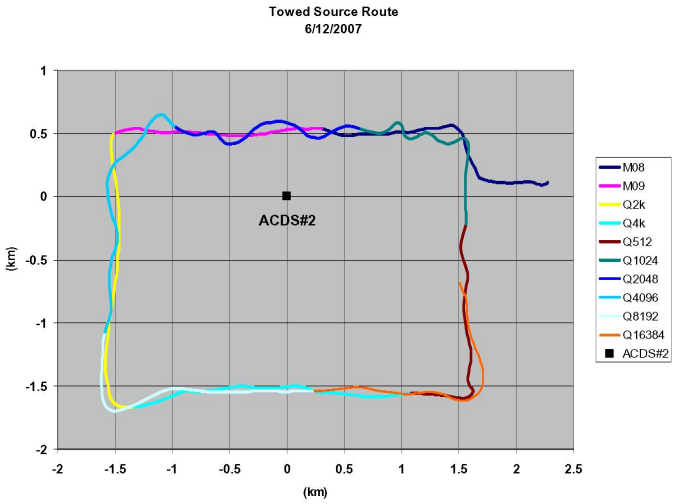

Fig. 3. The Route of the Towed Source around ACDS2. Experiments were conducted different data configurations. This paper presents results for QPSK modulated signal with the symbol block length $N = 512$.

Each transmitted packet consists of two Linear Frequency Modulation (LFM) waveforms, a 511-symbol m-sequence (Barker codes), and Quadrature Phase Shift Keying (QPSK) modulated data blocks, as shown in Fig. 4. The two LFM waveforms were 0.1 second chirps with off-set frequency ranging from -2 kHz to 2 kHz. The carrier frequency was 17 kHz and the signal bandwidth was 5 kHz. The symbol rate of the QPSK signal was 4 kilo-symbols per second and the pulse shaping and matched filters were the root raised cosine filter with a roll-off factor of 0.25. The gaps after the starting LFM and the m-sequence signal is long enough so that the channel Doppler shift can be estimated and symbol synchronization can be achieved. The gap after the ending LFM was designed to avoid inter-packet interference. The two LFM waveforms were used for Doppler shift estimation and time scaling estimation. The m-sequence was used for symbol synchronization. The total duration of a packet was 15 seconds.

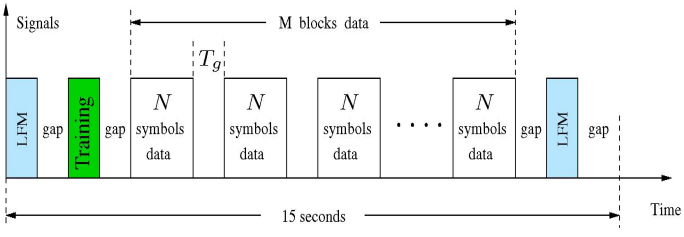

Fig. 4. Packet structure. Each packet contains M blocks of data, each data block contains P pilot symbols and $(N-P)$ information symbols.

The QPSK data signals were partitioned in M blocks each consisting of N symbols followed by a guard time T_g. The guard time T_g was sufficiently long to avoid inter block interference. The first data block was used as the pilot block for initial channel estimation. In each payload data block, P pilot symbols were also used for phase reference. Therefore,

978-1-4244-2126-8/08/$25.00 ©2008 IEEE

each packet contains $(M-1)(N-P)$ symbols of information data. The received data were recorded at a sampling rate of $F_s = 80$ kHz.

The algorithm for receiver data processing is presented in Section III and the results are presented in Section IV.

III. The Channel Equalization and Phase Correction Algorithm

A. System Model

Consider a SIMO underwater acoustic communications system with a single transducer source and N_r-hydrophone receiver. The transmitted baseband signal can be represented as

$$s(t) = \sum_{k=0}^{\infty} x(k) p_T(t - kT) \tag{1}$$

where T is the symbol interval, $p_T(t)$ denotes the transmit pulse shaping filter, and $x(k)$ the transmitted symbol at time instant k. The signal is modulated onto a single carrier and the passband signal can be written as

$$s_p(t) = \mathrm{Re}\left[\sum_{k=0}^{\infty} x(k) p_T(t - kT) \exp(j2\pi F_c t)\right] \tag{2}$$

where F_c is the carrier frequency. In the multipath and Doppler spread fading channel, assume a total number of I multi-paths at each hydrophone. The received passband signal at the m-th hydrophone $r_m(t)$ is

$$r_m(t) = \mathrm{Re}\left\{\sum_{i=0}^{I} A_{m,i} \sum_{k=0}^{\infty} x(k) p_T[(1+a_{m,i})t - kT - \tau_{m,i}] \times e^{[j2\pi(f_{m,i}+f_0+F_c)(t-\tau_{m,i})+j\phi_{m,i}]}\right\} + z_m(t) \tag{3}$$

where $z_m(t)$ is the additive white Gaussian noise (AWGN) and the parameters $A_{m,i}$, $\phi_{m,i}$, and $\tau_{m,i}$ are the gain, phase, and propagation delay of the i-th path and the m-th hydrophone, respectively. The Doppler f_0 is the average Doppler shift across all paths and hydrophones. The instantaneous Doppler drift of the (m,i)-th path is $f_{m,i}$, where $f_0 + f_{m,i} = a_{m,i}F_c$ and the Doppler scaling factor $a_{m,i} = \frac{v}{c}\cos\alpha_{m,i}$. Note v is the speed of the relative motion between the transmitter and the receiver, c is the speed of sound (approximately 1500 m/s), and $\alpha_{m,i}$ is the angle of arrival or departure of the (m,i)-th path.

At the receiver, the two LFM waveforms are used to estimate the average Doppler shift f_0 according to [10]. Then the carrier frequency off-set $a_0 F_c$ is applied to the demodulation, where $a_0 = E[\frac{v}{c}\cos\alpha_{m,i}]$ is the mean Doppler scaling factor. The demodulated signal is time scaled to compensate for signal dilation or compression and then down sampled to the symbol rate. The baseband equivalent signal received at the m-th hydrophone can be expressed in T-spaced sampling rate as

$$y_m(k) = \sum_{l=1}^{L} h_m(l,k) x(k+1-l) e^{j(2\pi f_{m,k} kT + \theta_{m,0})} + v_m(k) \tag{4}$$

where L is the fading channel length, T is the symbol interval, $f_{m,k}$ is the time-varying instantaneous Doppler drift, $\theta_{m,0}$ is the phase error after time scaling and symbol synchronization, and $v_m(k)$ is the additive noise with an average power of σ^2. The impulse response of the baseband equivalent channel $h(l,k)$ includes the effects of the transmit pulse-shaping filter, the physical time-varying channel response, and the receiver matched filter.

It is noted that the average Doppler shift is zero in fixed-to-fixed channels and the instantaneous Doppler drift is relatively small. In moving-to-fixed channels, the adopted demodulation method removes the average Doppler shift so that the baseband signal is similar to that of fixed-to-fixed channels. However, the instantaneous Doppler spread $f_{m,k}$ is usually larger resulting in more errors in channel estimation and equalization.

Adopting the zero-padding and overlap-add method [11] for N-point FFT, we define two signal vectors

$$\mathbf{x} = \begin{bmatrix} x(1) & x(2) & \cdots & x(N) \end{bmatrix}^t \tag{5}$$

$$\mathbf{y}_m = \begin{bmatrix} y_m(1) & \cdots & y_m(N_{zp}) & y_m(N_{zp}+1) & \cdots & y_m(N) \end{bmatrix}^t + \begin{bmatrix} y_m(N+1) & \cdots & y_m(N+N_{zp}) & 0 & \cdots & 0 \end{bmatrix}^t \tag{6}$$

where $N_{zp} = T_g/T > L$. The time-domain signals $\mathbf{x}$ and $\mathbf{y}_m$ are related as

$$\mathbf{y}_m = \mathbf{D}_m \mathbf{T}_m \mathbf{x} + \mathbf{v}_m \tag{7}$$

where $\mathbf{T}_m$ is a circulant matrix when the channel remains unchanged within a data block [7], and

$$\mathbf{D}_m = \mathrm{diag}\left\{e^{j(2\pi f_{m,1}T+\theta_{m,0})} \quad \cdots \quad e^{j(2\pi f_{m,N}NT+\theta_{m,0})}\right\} \tag{8}$$

$$\mathbf{v}_m = \begin{bmatrix} v_m(1) & \cdots & v_m(N_{zp}) & v_m(N_{zp}+1) & \cdots & v_m(N) \end{bmatrix}^t + \begin{bmatrix} v_m(N+1) & \cdots & v_m(N+N_{zp}) & 0 & \cdots & 0 \end{bmatrix}^t. \tag{9}$$

The frequency-domain representation of (7) is

$$\begin{aligned} \mathbf{Y}_m &\triangleq \mathbf{F}_N \mathbf{y}_m \\ &= \mathbf{F}_N \mathbf{D}_m \mathbf{F}_N^\dagger \mathbf{F}_N \mathbf{T}_m \mathbf{F}_N^\dagger \mathbf{F}_N \mathbf{x} + \mathbf{F}_N \mathbf{v}_m \\ &= \mathbf{\Phi}_m \mathbf{H}_m \mathbf{X} + \mathbf{V}_m \end{aligned} \tag{10}$$

where $\mathbf{X} \triangleq \mathbf{F}_N \mathbf{x}$. Equation (10) uses the FFT matrix property $\mathbf{F}_N^\dagger \mathbf{F}_N = \mathbf{I}_N$. The phase matrix $\mathbf{\Phi}_m = \mathbf{F}_N \mathbf{D}_m \mathbf{F}_N^\dagger$. Although $\mathbf{\Phi}_m$ is generally a non-diagonal matrix, the non-diagonal elements of $\mathbf{\Phi}_m$, *i.e.*, $\Phi_m(n,l)$ with $n \neq l$, are negligible comparing to the diagonal elements $\Phi_m(n,n)$. Its diagonal elements are equal to

$$\Phi_m(n,n) = \frac{1}{N}\sum_{k=1}^{N} e^{j(2\pi f_{m,k} kT + \theta_{m,0})}, \quad n = 1, 2, \cdots, N. \tag{11}$$

The frequency-domain channel response $\mathbf{H}_m$ is also diagonal if the channel coherence time covers the block duration, *i.e.*,

$$\begin{aligned} \mathbf{H}_m &= \mathbf{F}_N \mathbf{T}_m \mathbf{F}_N^\dagger \\ &= \mathrm{diag}\left\{H_m(1), \quad H_m(2), \quad \cdots, \quad H_m(N)\right\} \end{aligned} \tag{12}$$

with $H_m(n) = \sum_{l=1}^{L} h_m(l,1) \exp\left(\frac{-j2\pi(l-1)(n-1)}{N}\right)$.

978-1-4244-2126-8/08/$25.00 ©2008 IEEE

B. Channel Estimation and Equalization

The pilot block signals are used to estimate the fading channel. The frequency-domain representation (10) can be simplified as

$$\begin{aligned} Y_m(n) &= H_m(n)\Phi_m(n,n)X(n)+V_m(n) \\ &= \lambda_m H_m(n)X(n)+V_m(n),\ n=1,2,\cdots,N \end{aligned} \quad (13)$$

where $\lambda_m = \frac{1}{N}\sum_{k=1}^{N} e^{j(2\pi f_{m,k}T+\theta_{m,0})}$ is a complex-valued unknown parameter with its amplitude close to one.

The channel transfer function $\lambda_m H_m(n)$ is estimated by the minimum mean square error criterion as

$$\lambda_m \tilde{H}_m(n) = \frac{Y_m(n)X^*(n)}{|X(n)|^2+\sigma^2},\quad n=1,2,\cdots,N. \quad (14)$$

The estimate $\lambda_m \tilde{H}_m(n)$ can be further improved by a frequency-domain filter to reduce noise. The estimated channel response is applied to the next data block for channel equalization. Based on (10), the received signals at the N_r hydrophones can be expressed in the frequency domain as

$$\begin{bmatrix} \mathbf{Y}_1 \\ \mathbf{Y}_2 \\ \vdots \\ \mathbf{Y}_{N_r} \end{bmatrix} = \begin{bmatrix} \mathbf{\Phi_1 H_1} \\ \mathbf{\Phi_2 H_2} \\ \vdots \\ \mathbf{\Phi}_{N_r}\mathbf{H}_{N_r} \end{bmatrix} \mathbf{X} + \begin{bmatrix} \mathbf{V}_1 \\ \mathbf{V}_2 \\ \vdots \\ \mathbf{V}_{N_r} \end{bmatrix}. \quad (15)$$

Applying the MMSE criterion, we obtain the frequency-domain equalized block data as

$$\hat{\mathbf{X}} = \left(\sum_{m=1}^{N_r} |\lambda_m|^2 \hat{\mathbf{H}}_m^{\dagger}\hat{\mathbf{H}}_m + \sigma^2 \mathbf{I}_N\right)^{-1} \left(\sum_{m=1}^{N_r} \lambda_m^* \hat{\mathbf{H}}_m^{\dagger}\mathbf{Y}_m\right) + \hat{\mathbf{V}} \quad (16)$$

Applying the inverse FFT to the equalized data vector $\hat{\mathbf{X}}$, the equalized time-domain data vector $\hat{\mathbf{x}}$ is obtained as

$$\hat{\mathbf{x}} = \mathbf{F}_N^{\dagger}\hat{\mathbf{X}} \simeq \sum_{m=1}^{N_r} \left(\mathbf{F}_N^{\dagger}\mathbf{\Delta}_m\mathbf{F}_N\right)\mathbf{D}_m\mathbf{x} + \hat{\mathbf{v}}. \quad (17)$$

where

$$\mathbf{\Delta}_m = \left(\sum_{m=1}^{N_r} |\lambda_m|^2 \hat{\mathbf{H}}_m^{\dagger}\hat{\mathbf{H}}_m + \sigma^2\mathbf{I}_N\right)^{-1} \left(\lambda_m^* \hat{\mathbf{H}}_m^{\dagger}\mathbf{H}_m\right) \quad (18)$$

is a diagonal matrix due to the diagonal properties of $\{\hat{\mathbf{H}}_m\}_{m=1}^{N_r}$ and $\{\mathbf{H}_m\}_{m=1}^{N_r}$. It has been shown that the k-th symbol of $\hat{\mathbf{x}}$ can be approximated as

$$\begin{aligned} \hat{x}(k) &= \left[\sum_{m=1}^{N_r} \delta_m e^{j\left(2\pi f_{m,k}kT+\theta_{m,0}\right)}\right] x(k) + \hat{v}(k) \\ &= |\beta_k|\, e^{j\angle\beta_k} x(k) + \hat{v}(k) \end{aligned} \quad (19)$$

where $\beta_k = \sum_{m=1}^{N_r} \delta_m e^{j\left(2\pi f_{m,k}kT+\theta_{m,0}\right)}$ and $\delta_m = \frac{1}{N}\text{trace}\,(\mathbf{\Delta}_m)$.

Equation (19) clearly indicates that the equalized data symbol $\hat{x}(k)$ is an amplitude-scaled and phase-rotated version of the transmitted data symbol $x(k)$. When $x(k)$ is a PSK-modulated symbol, the time-varying rotating phase $\angle\beta_k$ must be compensated before detection.

C. Phase Correction and Symbol Detection

The rotating phase $\angle\beta_k$ is a combined effect of the symbol synchronization, time-scaling errors, and time-varying Doppler drifts of the N_r fading channels. Since the instantaneous Doppler $f_{m,k}$ changes gradually over a short period of time, the rotating phase $\angle\beta_k$ also changes gradually without abrupt jumps. Therefore, we use P pilot symbols at the beginning of each payload data block to facilitate the initial phase estimation. We then partition the data block into small groups of N_s symbols/group, estimate the average phase drift of the group, and remove the phase rotation from (19). The details of the phase correction algorithm may be found in [7].

For fixed-to-fixed channels, the number of pilot symbols maybe selected as small as two and the BER performance of the algorithm is on the order of 10^{-4}. For moving-to-fixed channels, more pilot symbols are required to achieve a similar performance.

IV. Results

Thirty-six data packets of the moving-to-fixed channel experiment were processed. The parameters of the data signals were: the number of receive hydrophone was $N_r = 8$, the block size $N = 512$, the number of blocks in a packet $M = 86$, the number pilot symbol in each data block for phase estimation $P = 8$, the group size $N_s = 16$, and the total number of information bits in a packet was 85680. The multipath fading channel length was estimated to span 5 ms and the length of the equalizer was chosen as $L = 20$. Since the channel coherence time is about 100 ms, the channel impulse responses were re-estimated in every data block using the detected symbols and the updated channel was used in the next data block for equalization. Symbol synchronization was achieved using the m-sequence with 2 samples/sybmol for better accuracy. Improved BER performance was also achieved using $2N$-point FFT according to [12] over N-point FFT. The BER performances of some representative packets are presented in Tables 1 – 3, along with their estimated Doppler shifts and maximum Doppler drifts. Among the 36 packets, 14 packets achieved excellent BER of less than 1×10^{-3}, 20 packets achieved a BER between 1×10^{-3} and 1×10^{-2}, and two packets performed worse than 1×10^{-2}. The overall average BER is 1.81×10^{-3}.

Table 1: Fourteen of the 36 packets achieved BER $< 10^{-3}$ without coding. Eight packets are listed.

Packet Identifier	Bit Error Rate	Ave. Doppler Shift (Hz)	Max Doppler Drift (Hz)
163140516	$2.27E-04$	7.1884	± 2
163140546	$5.11E-04$	12.7280	± 2
163141317	$6.81E-05$	8.1703	± 1.5
163141532	0	7.0052	± 1
163141547	$2.95E-04$	7.9284	± 3
163141631	$4.54E-05$	11.5483	± 2
163141716	$7.95E-05$	10.3685	± 2
163141917	$4.54E-05$	-4.1767	± 1

978-1-4244-2126-8/08/$25.00 ©2008 IEEE

Table 2: Twenty of the 36 packets achieved $10^{-3} <$ BER $< 10^{-2}$ without coding. Eight packets are listed.

Packet Identifier	Bit Error Rate	Ave. Doppler Shift (Hz)	Max Doppler Drift (Hz)
163140031	$1.90E-03$	-14.4060	± 4
163140047	$1.31E-03$	-15.1681	± 4
163140601	$1.06E-03$	17.4470	± 4
163140702	$1.20E-03$	8.0164	± 2
163141231	$2.20E-03$	10.5664	± 3
163141602	$1.40E-03$	8.8444	± 3
163141646	$1.70E-03$	11.5849	± 4
163141802	$1.20E-03$	7.1517	± 3

Table 3: Two of the 36 packets performed worse than 10^{-2} without coding. All packets are listed.

Packet Identifier	Bit Error Rate	Ave. Doppler Shift (Hz)	Max Doppler Drift (Hz)
163140401	0.0144	-8.9690	± 4.5
163140532	0.0151	13.2116	± 4.5

The channel coherence time was estimated by the m-sequence transmitted in the M09 run and the result is shown in Fig. 5. It is clear that the coherence time is about 100 ms which is smaller than the duration of a data block. This indicates that the channel re-estimation is necessary for each data block.

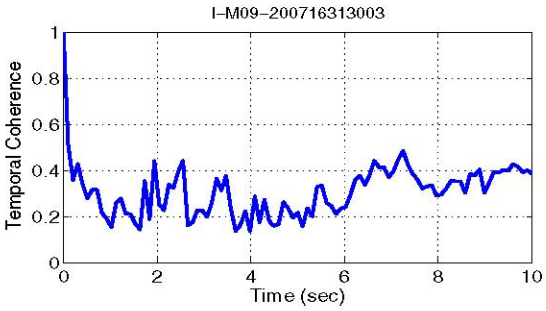

Fig. 5. Typical channel temporal coherence estimated by m-sequence in the M09 run of the experiment. The channel coherence time was approximately 100 ms at the 0.5 coherence level. This was smaller than the duration of a data block of 132.5 ms.

A typical frequency response estimated by the pilot block or detected data blocks is plotted in Figs. 6, where the top figure shows the response without noise reduction and the response exhibits many spikes. The bottom figure is the coefficients filtered in the frequency domain and is free of spikes. The noise-reduced responses were used for channel equalization to improve the performance.

The estimated time-varying Doppler drift and initial phase drifts are shown in Fig. 7. It is noted that the isolated spikes are due to the re-estimation of the channel parameters, which leads to a phase jump between currently estimated channel parameters and the previously estimated channel parameters. Although the Doppler drift varies between -4.5 Hz and 4.5 Hz, its average value in each packet is almost zero after

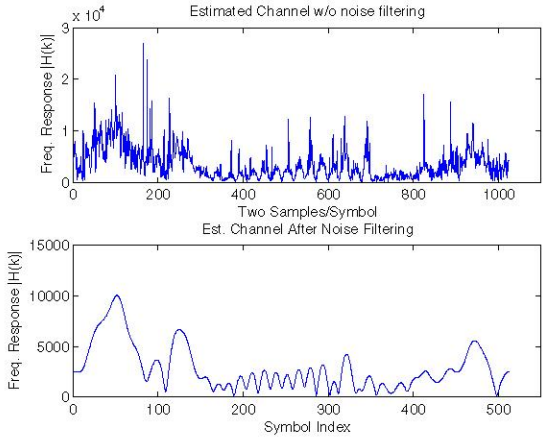

Fig. 6. The estimated channel responses with and without noise reduction.

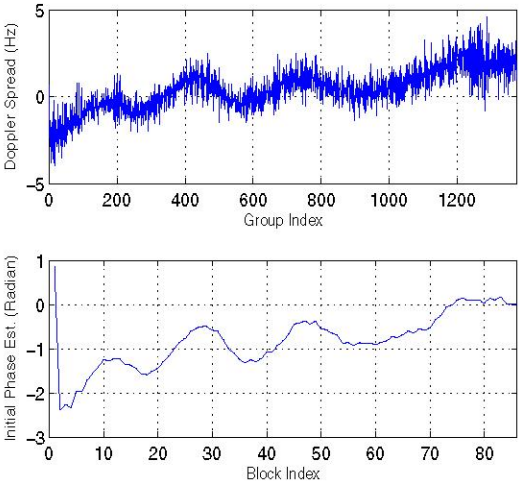

Fig. 7. Doppler drift and initial phase estimation. Each block of data is partitioned into 16 groups and each packet has 86 blocks.

compensating for Doppler shift at the demodulation stage. This time-varying Doppler spread will lead to individual data symbol to be compressed or dilated.

The BER distributions across a packet were also investigated and typical distributions are plotted in Fig.8–Fig.10. For the packets that achieved an overall BER $< 10^{-3}$, a few errors were found randomly distributed in several blocks across the packet. Each error block contained less than two error bits, as shown in Fig.8. Note that each data block contains 1008 information bits and a packet contains 85680 information bits. For those packets that achieved a good overall BER between 10^{-2} to 10^{-3}, some blocks contained 1% to 5% error bits, as shown in Fig.9. For the three packets that had a BER higher than 10^{-2}, some blocks contained 10% to 35% error bits, as shown in Fig.10. The bit errors were mainly caused by channel estimation errors that was accumulated in a few blocks, but it seemed to self-heal after a few blocks. The reason for this behavior is yet to find out.

978-1-4244-2126-8/08/$25.00 ©2008 IEEE

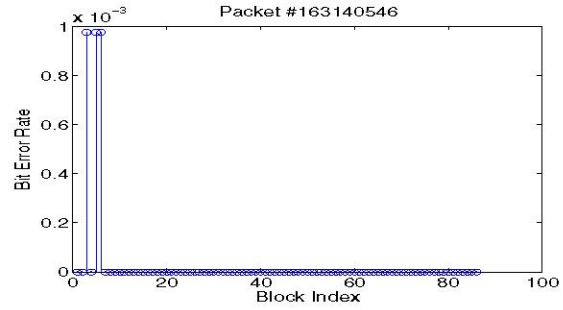

Fig. 8. Typical BER distribution across data blocks for those packets that achieved an excellent overall BER $< 10^{-3}$. A few errors were found randomly distributed in several blocks across the packet. Each error block contained less than two error bits.

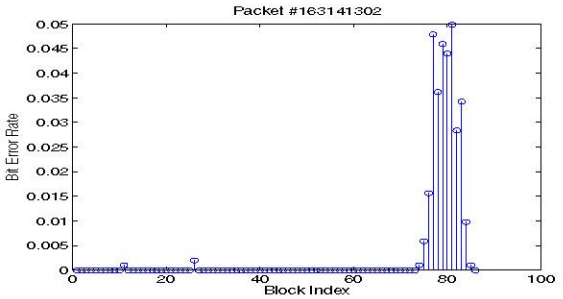

Fig. 9. Typical BER distribution across data blocks for those packets that achieved a good overall BER between 10^{-2} to 10^{-3}. Some blocks contained 1% to 5% error bits.

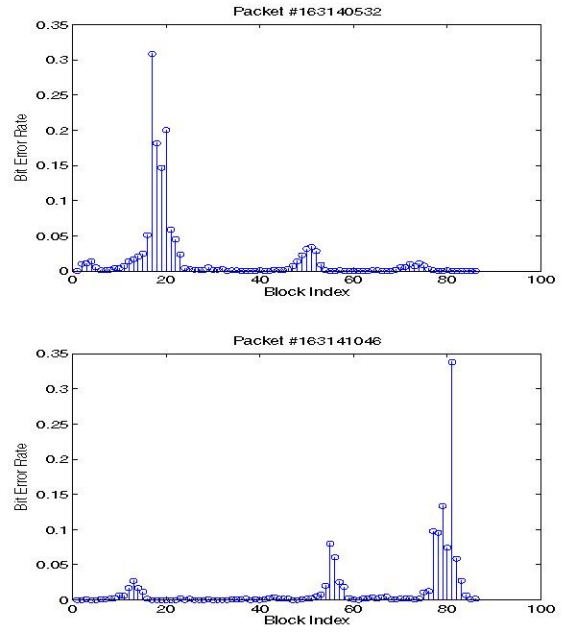

Fig. 10. BER distribution across data blocks for those packets that achieved an overall BER worse than 10^{-2}. Some blocks contained 10% to 35% error bits. The channel estimation and equalization seemed to self-heal after making a large number of errors in a bad block. The reason of this behavior is yet to be found.

V. Conclusion

The frequency-domain channel equalization and phase correction method has been applied to moving-to-fixed channels in the AUVFest'07 ocean experiment. The moving source channels exhibit higher Doppler shift and larger Doppler drift than the fixed-to-fixed channels. Therefore, the number of symbols required for initial phase estimation has been increased from 2 to 8 symbols when the group-wise phase correction algorithm is applied to moving sources. Thirty-six packets with QPSK modulation and a data block length of 512 have been processed and 34 of them achieved a BER better than 10^{-2}. The overall uncoded BER performance of all 36 packets is 1.81×10^{-3} which is slightly higher than that of fixed-to-fixed channels. Further improvement can be made through coding schemes or better accuracy in Doppler estimation and channel/symbol synchronization.

Acknowledgments

This work was supported in part by the Office of Naval Research under Grant N00014-07-1-0219 and the National Science Foundation under Grant CCF-0514770. The work of T. C. Yang and W.-B. Yang was supported by the Office of Naval Research.

References

[1] M. Stojanovic, J. Catipovic, and J. Proakis, "Phase-coherent digital communicaitons for underwater acoustic channels," *IEEE J. Ocean Eng.*, vol.19, pp.100-111, Jan. 1994.

[2] T. H. Eggen, A. B. Baggeroer, and J. C. Preisig, "Communication over Doppler spread channels – Part I: channel and receiver presentation," *IEEE J. Ocean Eng.*, vol.25, pp.62-71, Jan. 2000.

[3] T. C. Yang, "Differences between passive-phase conjugation and decision-feedback equalizer for underwater acoustic communications," *IEEE J. Ocean Eng.*, vol.29, pp.472-487, April 2004.

[4] T. C. Yang, "Correlation-based decision-feedback equalizer for underwater acoustic communications," *IEEE J. Ocean Eng.*, vol.30, pp.865-880, Oct. 2005.

[5] H.C. Song, W.S. Hodgkiss, W.A. Kuperman, M. Stevenson, and T. Akal, "Improvement of time-reversal communications using adaptive channel equalizers," *IEEE J. Ocean Eng.*, vol.31, pp.487-496, Apr. 2006.

[6] J.A. Flynn, J.A. Ritcey, D. Rouseff, and W.L.J. Fox, "Multichannel equalization by decision-directed passive phase conjugation: experimental results," *IEEE J. Oceanic Eng.*, vol.29, pp.824-836, July 2004.

[7] Y. R. Zheng, C. Xiao, T.C. Yang, and W.B. Yang, "Frequency-domain channel estimation and equalization for single carrier underwater acoustic communications," *MTS/IEEE Int. Oceans Conf.*, Vancouver, Canada, Sep., 2007.

[8] Y. R. Zheng, "Channel Estimation and Phase-Correction for Robust Underwater Acoustic Communications," *IEEE Int. Military Conf.*, Orlando, FL, Oct., 2007.

[9] T. Walzman and M. Schwartz, "Automatic equalization using the discrete frequency domain," *IEEE Trans. Info. Theory*, vol.IT-19, pp.57-68, Jan. 1973.

[10] B. S. Sharif, J. Neasham, O. R. Hinton, and A. E. Adams, "A computationally efficient Doppler compensation system for underwater acoustic communications," *IEEE J. Ocean Eng.*, vol.25, pp.52-61, Jan. 2000.

[11] B. Muquet, Z. Wang, G. Giannakis, M. de Courville, and P. Duhamel, "Cyclic prefix or zero padding for wireless multicarrier transmissions?" *IEEE Trans. Commun.*, vol.50, pp.2136-2148, Dec. 2002.

[12] M. V. Clark, "Adaptive frequency-domain equalization and diversity combining for broadband wireless communications," *IEEE J. Select. Areas Commun.*, vol.16, pp.1385-1395, Oct. 1998.